1 MUON STORAGE RING

This file is parkerCh16ver10.tex Except in figures colored text denotes editorial information which should be omitted from the final document.

In the Study–I report this is Section 8 but for Study–II it should be renamed Section 16. For this draft the headings from Study–I have been incorporated then modified.For comparison details please refer to Study–I.

For this first draft some of the figures were already modified to be consistent with a later optimized lattice configuration denoted mu_mf11c1 rather than the mu_mf09b lattice presented at the January 29 editors meeting. The new lattice has:

- Larger beta functions in the production straight, which which are needed to meet the experiments beam divergence goal of 0.1 normalized divergence.
- Smaller peak horizontal dispersion, which reduces the horizontal aperture requirements for $\pm 2.2\%$ in the dispersion suppressor enough to be able to use a conventional normal conducting quadrupole in the empty cell.

On advice from Scott Berg I will drop back to the mu_mf09b baseline lattice and only look to accept $\pm 1.9\%$ momentum spread, which is another way to keep the empty cell aperture requirement small. However this does not address the issue that the optics contribution from the production straight to the neutrino beam angular spread is about 30% too high. Fig. 2 and Fig. 6 will be revised accordingly. B.P.

1.1 Introduction

B. Parker

For Study–II the muon storage ring has a simple planar racetrack configuration as shown in Fig. 1. The racetrack is tilted such that the downward going straight section, denoted the production straight, is aimed at the distant neutrino detector. For a BNL site, depending on ring size, some of the racetrack will probably be above ground level due to the desire to keep the lowest part of the ring above the local water table. The aboveground region will be covered with fill material, mostly sand, and thus there is an incentive to keep the long axis of the racetrack as short as possible to reduce the required fill volume. This arrangement does make it much easier to inject beam into in the upward going return straight section than was possible for the completely below ground placement considered in Study–I.Injecting into specially tailored reduced-beta optics in the return straight section rather than the high-beta optics needed in the production straight dramatically eases the injection system requirements compared to Study–I as will be discussed later.

Since the fraction, f_s of muon decays which makes neutrinos which are aimed toward the detector is $f_s = L_s/C = L_s/(2L_s + L_{Arc})$, with C the ring circumference and L_{Arc} the length of one arc, it is clear that creating the shortest possible arc maximizes f_s and keeps the ring footprint as small as possible.

Because the present ring energy is 20 GeV compared to the Study–I 50 GeV, a naive expectation is that for the same f_s the Study–II ring circumference should be $\frac{2}{5}$ the Study–I circumference of 1753 m or about 700 m. In practice it is hard to achieve this scaling. Even if one takes a larger

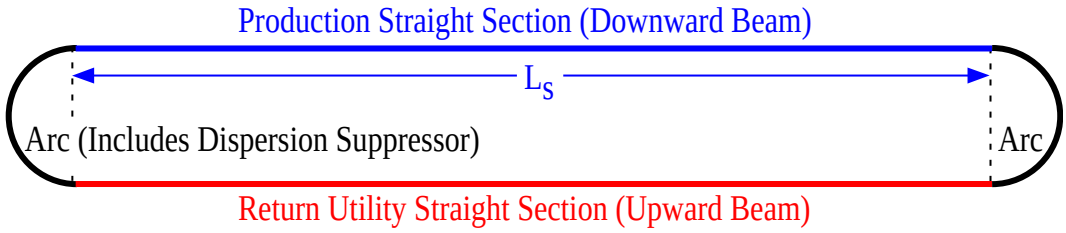

Figure 1: Sample Figure.

dipole field, 7 T instead of the Study–I 6 T, it is hard to make the basic separated function arc cell much shorter. As indicated in Fig. 2 shortening the individual magnets only serves to reduce the magnetic packing fraction since the coil ends cannot be arbitrarily shortened. In fact for a lower beam energy a larger magnet aperture is needed, assuming equal lattice functions and normalized emmitance, and thus the coil ends should be made even longer than for the Study–I magnets.

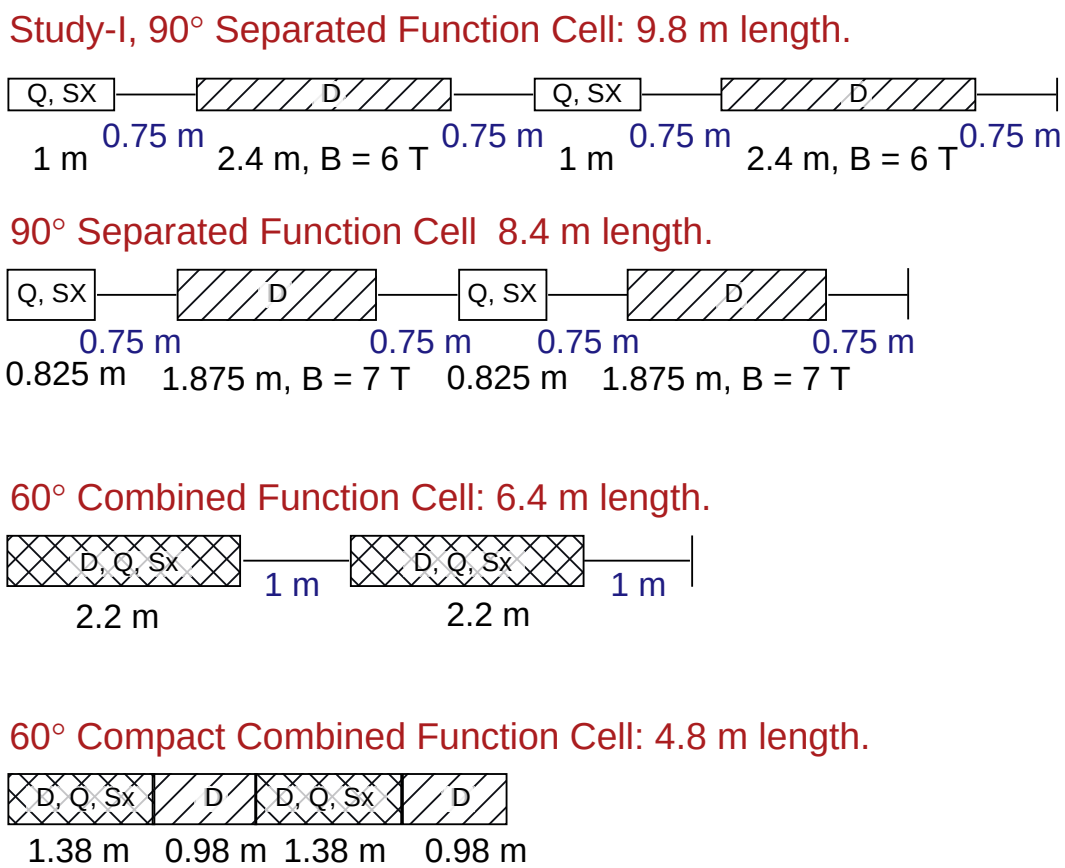

Figure 2: Sample Figure.

With a separated function focusing cell the only path left to make a short 20 GeV arc is to make the arc up from fewer cells than were used for Study–I and inevitably the bend angle per cell is increased. Unfortunately a larger bend angle per cell leads to larger peak dispersion which in turn implies a need for even more magnet aperture to handle the muon beam's large momentum spread.

We did find it possible to shorten the arc cell by using combined function magnets. As indicated in Fig. 2 even with a somewhat smaller dipole guide field, reduced to accommodate the superposition of quadrupole and dipole fields at the conductor, and a more relaxed intermagnet spacing, it is feasible to shorten the basic arc cell and achieve a circumference below the naive 700 m scaling prediction.

Two possible ways to implement such a combined function field configuration, the first with $\cos n\theta$ coils and the second with flat pancake coils are show schematically in Fig 3. The pancake coil configuration is especially interesting because its simple bend structure enables us to use a brittle prereacted superconducting material, such as Nb_3Sn for making a high field magnet. Also an open coil structure helps to avoid energy deposition from decay electrons which are swept by the guide field to smaller bend radius in the magnet's midplane.

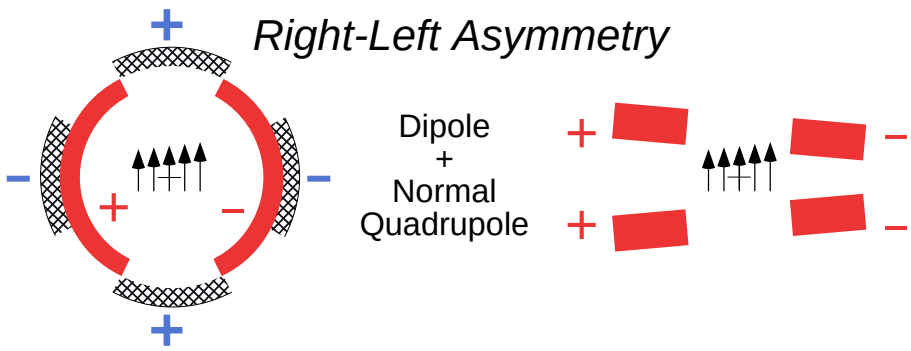

Figure 3: Sample Figure.

In addition to conventional upright quadrupole focusing we also investigated focusing structures using a combination of skew quadrupole and normal dipole fields. As indicated in Fig. 4 and Fig. 5 such skew quadrupole can naturally be made with various arrangements of either $\cos n\theta$ or pancake coils. The skew quadrupole gradient is independently adjustable from the dipole component in Fig. 4 and fixed via coil geometry in Fig. 5. Skew combined function focusing implies top-bottom asymmetry while upright combined function focusing come from right-left coil asymmetry.

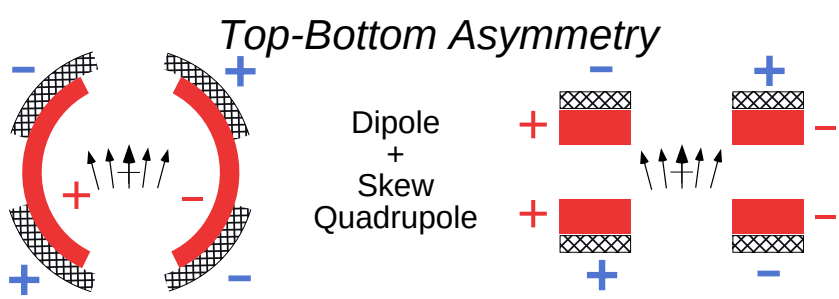

Figure 4: Sample Figure.

There is however one trick which only works for making skew quadrupole fields, displacing the coil ends longitudinally with respect to the dipole body field. This trick is illustrated in Fig. 6.

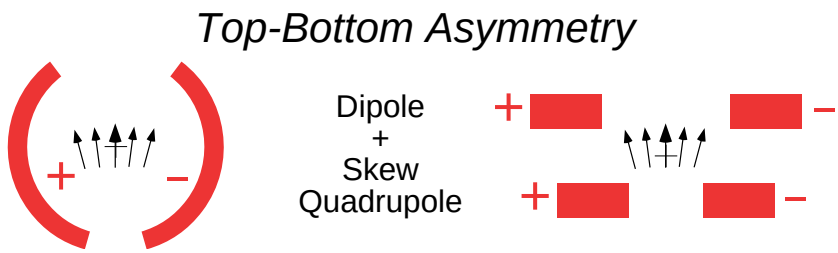

Figure 5: Sample Figure.

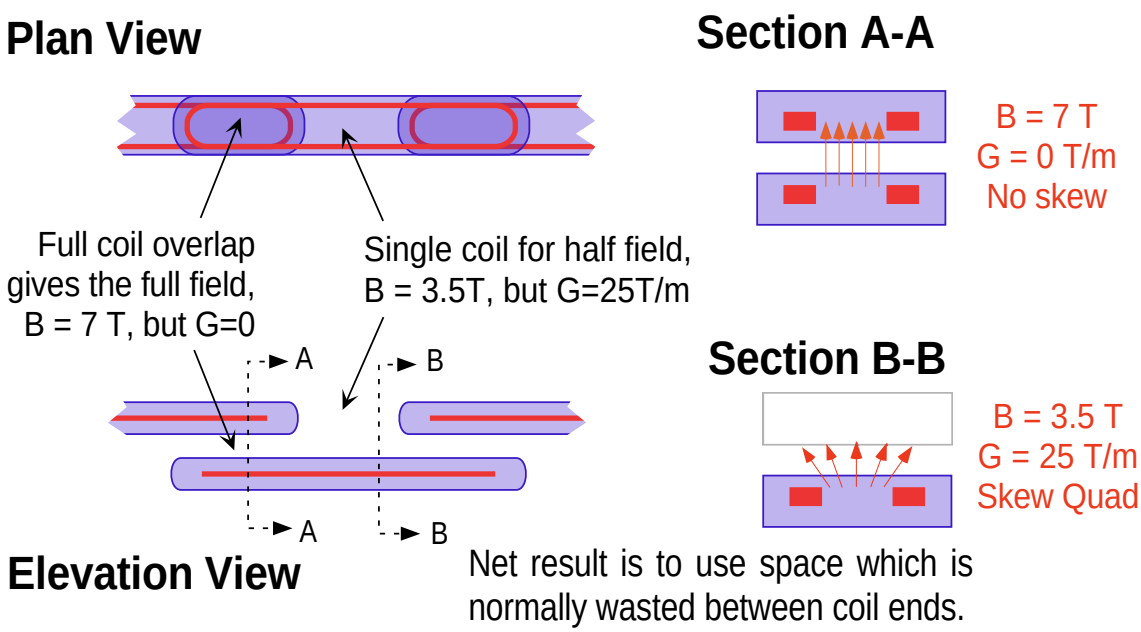

Figure 6: Sample Figure.

By changing the top-bottom overlap of the pancake coils, as indicated schematically in Fig. 6, we create double coil regions with the full dipole field but no skew focusing which alternate with single coil gap regions with roughly half the dipole field but full skew quadrupole focusing. The sign of the skew quadrupole focusing depends upon whether the top or bottom coil is missing in the single coil gap region. The result is a compact magnet structure with quasicontinuous bending and alternating gradient focusing. This new focusing structure can be made more compactly than is possible with a standard combined function cell because the space penalties which come from magnet coil ends are essentially avoided and therefore this compact skew focusing cell structure is the basis for the Study–II muon storage ring lattice.

1.2 The Lattice

B. Parker

Lattice functions for the 20 GeV muon storage ring using compact skew combined function arc cells are shown in Fig. 7. Here the beta functions, (β_A, β_B) are given for the 45° rotated betatron

eigenplanes (A,B) shown in Fig. 8 but the eigenplane dispersion functions (η_A, η_B) are projected to dispersion in the normal horizontal-vertical, (β_X, β_Y), coordinate system according to the relation ships, $\eta_X = \frac{\eta_A + \eta_B}{\sqrt{2}}$ and $\eta_Y = \frac{\eta_A - \eta_B}{\sqrt{2}}$.

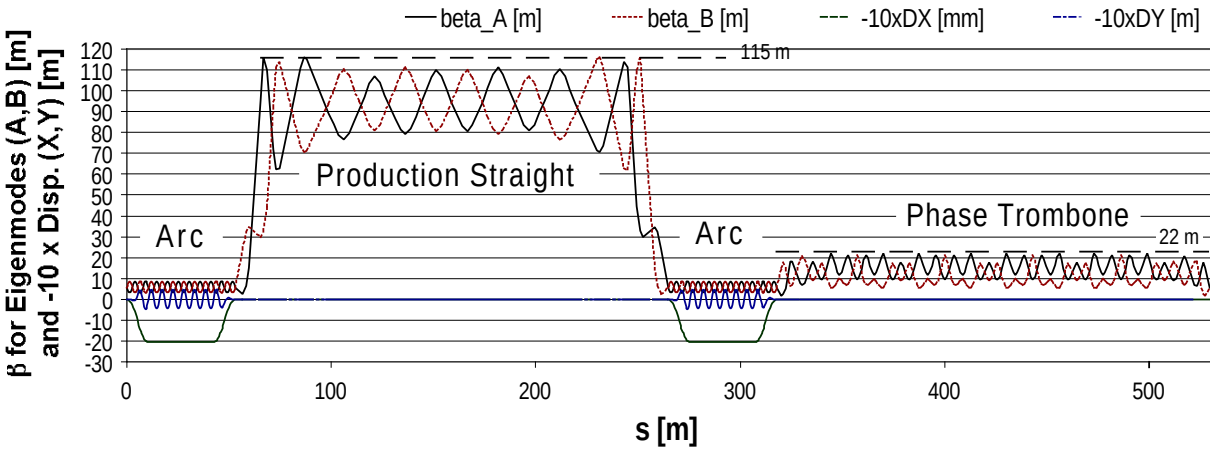

Figure 7: Sample Figure.

By construction the dispersion in the A and B eigenplanes is nearly equal so the effective vertical dispersion is much smaller than the horizontal dispersion. With this skew lattice the horizontal dispersion is nearly constant across the arc while the vertical dispersion oscillates with small amplitude about zero. Each arc contains cells without bending such that with 60° cell phase advance the dispersion is matched to zero for both eigenplanes in the straight sections.

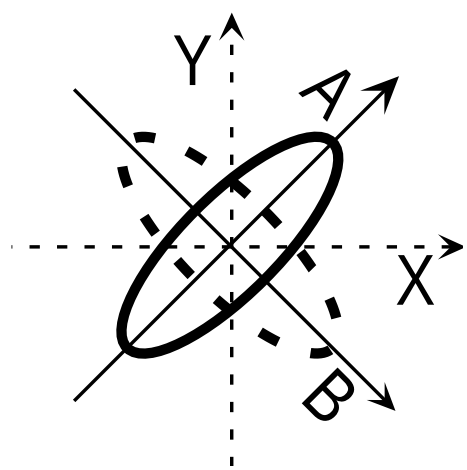

Figure 8: Sample Figure.

The lattice shown in Fig. 7 has a 1:4 length ratio between the lengths of arcs and straight sections in order to have a geometric decay ratio, f_s, equal of 40%. The production straight beta functions are large in order limit the impact of the muon beam divergence on the divergence of the neutrino beam and the beta functions in the return straight are intermediate in magnitude between the values in the arcs and production straight in order to simplify injection.

Symmetry between the (A,B) betatron eigenplanes is ensured by requiring a small added normal quadrupole focusing component, with normalized strength, K_ρ, $K_\rho = -\frac{1}{2\rho^2}$ in order to partially offset the weak focusing due to a sector dipole bend of local bend radius, ρ. As discussed in a paper by Byrd, Sagen and Talman[2] if left uncompensated the weak normal focusing of a sector bend shows up as coupling between the otherwise uncoupled independent betatron motion in the (A,B) eigenplanes. The value chosen above for K_ρ is precisely the amount needed to make the weak normal focusing in the linear lattice cylindrically symmetric and thus to restore symmetry between the (A,B) eigenplanes.

In practice K_ρ of order parts per mil of the skew focusing strength, K_S, is sufficient to ensure local linear decoupling. Note that the addition of K_ρ does not cancel the weak sector focusing and the net focusing in an arc cell with bending is slightly different from than of a cell without bending. Accounting for this difference is important for getting a good dispersion match. Also for nonzero momentum offset, $\Delta p/p$, one has to be prepared to deal with coupling effects due to expected nonlinear edge fields.

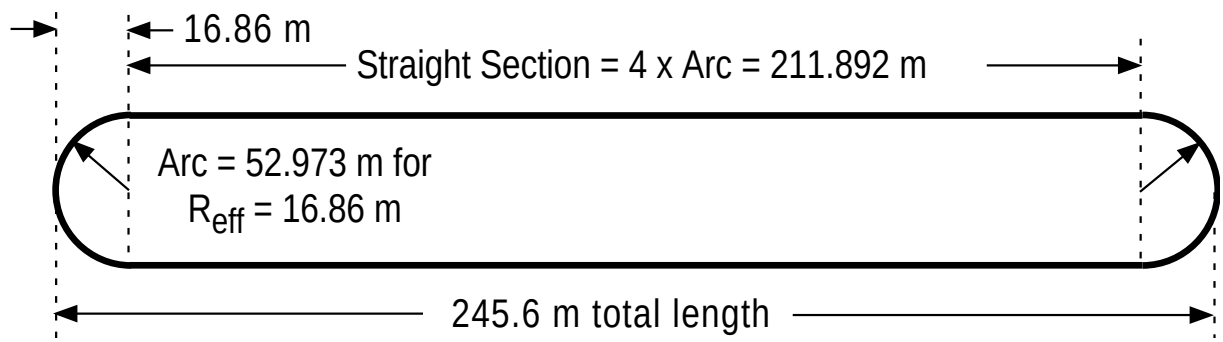

Figure 9: Sample Figure.

The ring geometry is shown in Fig. 9. The arcs at the racetrack ends are each end are 53 m long and for f_s = 40% we have the straight sections at four times this length at 219 m for a circumference which is ten times the single arc length or 530 m. Defining the effective arc radius, $R_{eff} = L_{Arc}/\pi$ gives R_{eff} = 16.9 m for a total machine length of 246 m. Depending upon the location of the neutrino detector, which affects the racetrack dip angle, it may be desirable to shorten the straight sections somewhat. This strategy helps to reduce the amount of fill needed for a steep dip angle at the cost of smaller f_s.

The Arcs B. Parker

The arc lattice is shown in more detail in Fig. 10. The arc contains ten 60° cells for a total phase advance across one arc of $\frac{10}{6}$ in both eigenplanes. With the chosen 60° phase advance it is possible to match to zero dispersion by omitting the dipole field component from the second and next to last arc cells. The focusing skew quadrupoles in these empty cells will be done with conventional warm skew quadrupoles while the rest of the arc is made up from the regular pattern of overlapping pancake superconducting coils supported in a warm iron yokes described earlier. Magnetic field and arc cell optics parameters are listed in Table 1.

Beam profiles near the beginning and end of the arcs, where the beam size contribution due to

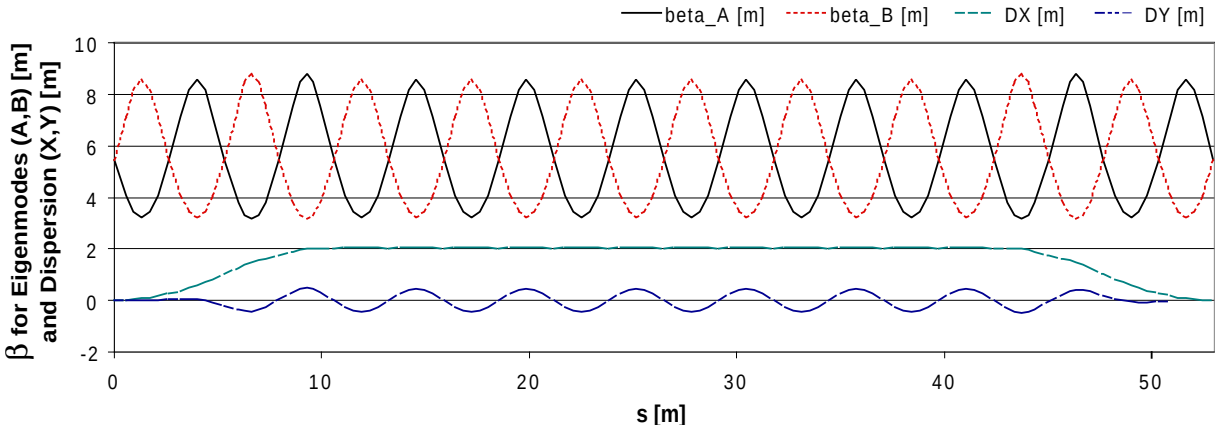

Figure 10: Sample Figure.

Table 1: Arc magnet and optics parameters table (blank).

AAA	BBB	CCC

dispersion is negligible, are shown at a skew defocusing location in Fig. 11 and a skew focusing location in Fig. 12.

Near the middle of the full dipole region, where there are both top and bottom coils the beam profile is round as shown in Fig. 13

Will include description of skew sextupole chromaticity correction scheme as well as a description of how to break the regular coil pattern at transitions to empty cell regions and at the ends of the arc (this requires some short coils). Note that discussion of ways to make optics adjustments and beam orbit bumps (e.g. corrector magnets) is beyond the present scope of work but could reasonably be argued as needed under a heading of beam commissioning or operational scenarios. Also the design of the skew sextupoles is presently not addressed.

Magnet design details for warm and cold magnets will be given in later subsections.

Production Straight B. Parker

Physics requirements drive large beta functions. Possible additional topics for this section in-

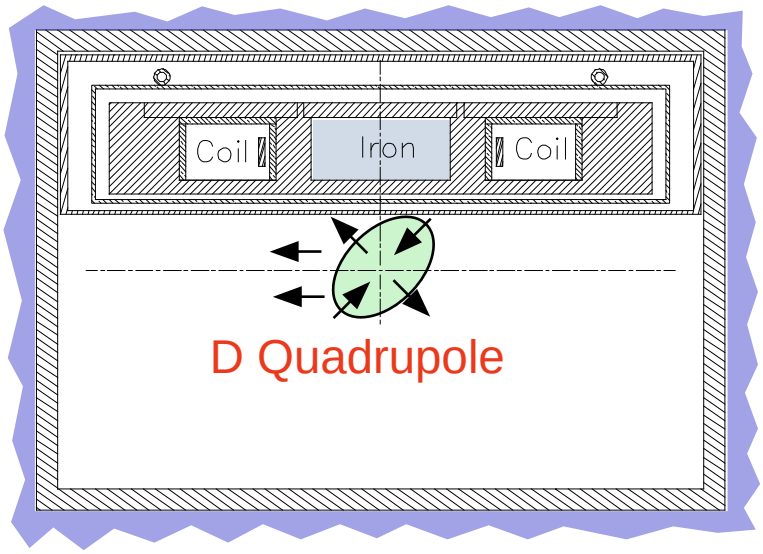

Figure 11: Sample Figure.

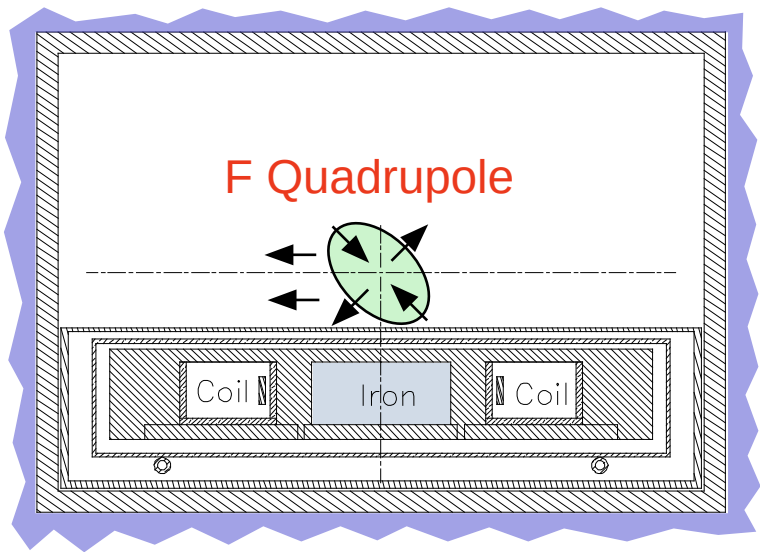

Figure 12: Sample Figure.

clude: discussion of rf system requirements and possible normal quadrupole decoupling scheme.

Return Straight B. Parker but maybe C. Johnstone is better here?

During the editors meeting only a place holder was described for this region. It makes sense to me to outline the functional requirements for this straight section but try to avoid being too specific about the actual detailed solution as this is the only straight section left where we can introduce knobs to fix problems elsewhere. One difference with Study–I is that it does look reasonable to inject going up into the return straight and this should be much more favorable than trying to inject into the high beta production straight.

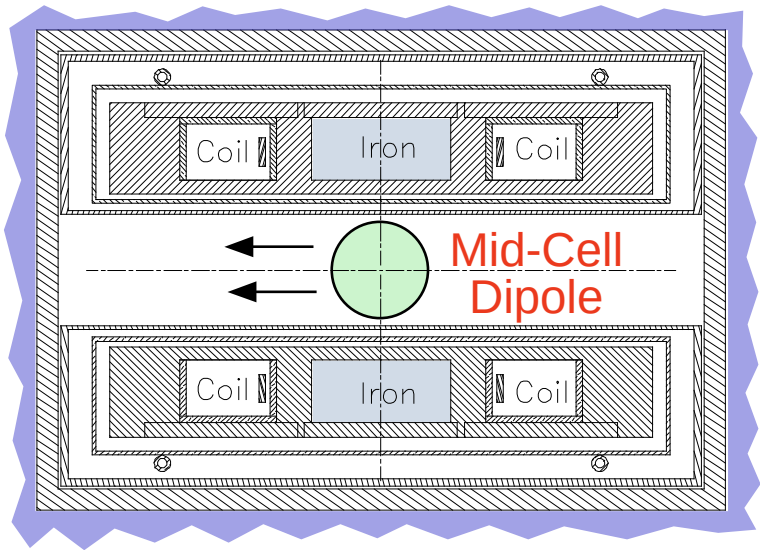

Figure 13: Sample Figure.

In conversations with Scott Berg it seems that it may not be necessary to have rf-cavities (if momentum compaction is small enough that beam does not spread out too much during a few hundred turns). Could include short section here on parameters for a minimal rf-system to keep beam from debunching. Note that if one follows Lebedev's suggestion to use a 200 MHz cryomodule of the same type as in his accelerator proposal then we will have to face up providing high quality vacuum near the superconducting cavities (presumably without the use of his isolation windows).

Ring Acceptance B. Parker

For calculation the effective vertical betatron acceptance, β_{eff}, we have $\beta_{eff} = \frac{\beta_A+\beta_B}{2}$ and for half aperture, Δh, as shown in Fig. 14 we have physical acceptance, A, of $A = \frac{(\Delta h)^2}{\beta_{eff}}$ or normalized acceptance, A_n, $A_n = \gamma A$. Values are given in Table 2

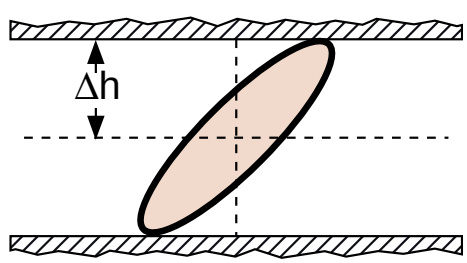

Figure 14: Sample Figure.

As show schematically in Fig. 15 a pencil beam with momentum offset, $\Delta p/p$, moves the beam horizontally by an amount, ΔX, $\Delta X \approx \eta_X \times \Delta p/p$ and vertically by an amount, ΔY, $\Delta Y \approx \eta_Y \times \Delta p/p$. Values are given in Table 3

If we use a round beam pipe in the warm skew quadrupoles in the production straight section, as shown in Fig. 16, we see that the betatron acceptance can be calculated directly from the eigenplane

Table 2: Betatron acceptance in the arcs.

AAA	BBB	CCC

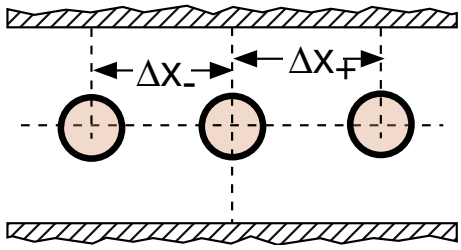

Figure 15: Sample Figure.

beta functions, (β_A, β_B), as shown in Table 4.

It is probably desirable to use a butterfly or other shape beam pipe in some of the skew quadrupoles that the injected beam goes through off axis as this is a relatively cheap way to gain a bit of injection aperture.

Injection System B. Parker

Without some better idea for the transfer line it is hard to be too specific here. We should be able to show a straw design for estimates of magnet parameters, required apertures etc. Must decide: Should we discuss magnetic septum quadrupole and should we include a description of collimation system for protection against injection errors here?

It may make sense to postpone discussion of the beam protection components to the later energy deposition section. Nikolai?

Superconducting Magnets ?

Conventional Warm Magnets B. Parker

This section covers: the warm quadrupoles in the arcs, optics matching quadrupoles near ends of the straight sections and the straight section quadrupoles. If time permits we may want to

Table 3: Momentum acceptance in the arcs.

AAA	BBB	CCC

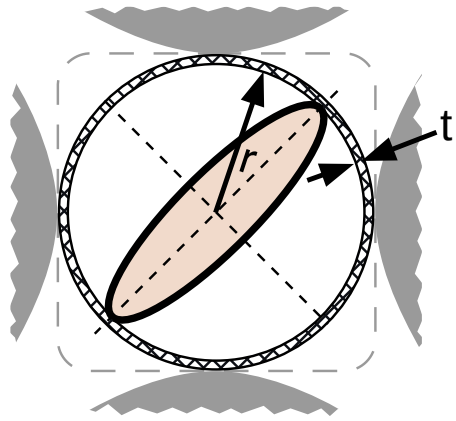

Figure 16: Sample Figure.

Table 4: Betatron acceptance in the production straight.

AAA	BBB	CCC

include some requirements for beam orbit control corrector dipoles, ring tune and coupling control quadrupoles.

Anything else, Carol?

Instrumentation J. Norem

The cooling ring presents some new beam instrumentation problems. In addition to the usual emittance, divergence, closed orbit, injection, extraction, beam loss and beam energy measurements, it seems desirable to measure the beam polarization, and precision measurements of beam direction in the decay straight section as a function of time, to help determine the parameters of the neutrino beam. The instrumentation issues for the muon beam in the storage ring should utilize mostly proven technology. The primary difficult would be that precision measurements can be complicated by the presence of decay electrons in the beam.

The muon decays can help determine some of the machine parameters. Semertzidis and Morse[1] have looked at using the $g-2$ frequency of the muons to determine the beam energy. They consider measurement of the synchrotron radiation from decay electrons which will give a very substantial signal.

We anticipate that the 6D "pencil" beams used to tune up the accelerator will also be useful in tuning up and operating the storage ring.

One issue which has been identified is the possibility of a high electron shower background at the downstream end of the two straight sections. This background would be due to muon decay electrons which were not swept from the beam. Although the fraction of primary decay electrons in the beam is $L/\gamma\tau c$, where L is a path length in the storage ring, and $\gamma\tau c \sim 126$ km, is the decay

length at 20 GeV. This means the fraction of muons which will decay in the 116 m straight sections is 0.001, and the electron/muon ratio at the downstream end of the straight will be $\sim 0.001 F_s$, where F_s is a factor which depends on the probability of electrons being swept and showering in the vacuum pipe. Estimates of the electron background are underway, but it seems desirable to consider precision measurements external to the ring for determining the neutrino beam direction, profile and divergence.

We assume the most reliable measurements of the neutrino beam size and divergence would be obtained from fine grained detector consisting of Tungsten sheets interspersed with hodoscopes. These would be located in shafts downstream of the decay straight. Rates could be high, on the order of 100 events/fill for a 1 m detector. (more details coming - M. Goodman)

More detailed descriptions of polarization measurements and other neutrino measurements will be added in a later draft.

Power Supplies for the Muon Storage Ring No name
To this point no new work done here so everything has to be TBD.

Quench Protection Dumps No name
To this point no new work done here so everything has to be TBD.

Muon Storage Ring Quench Detection and Protection No name
To this point no new work done here so everything has to be TBD.

1.3 Lattice Performance and Tracking

C. Johnstone

The issues discussed here are similar to those from Study–I but in detail things will look quite different due the novel features of the proposed skew focusing lattice.

A description of the on going work with Kyoko Makino, Martin Berz etc. belongs here. The importance of this work is such that it could point to the need for reworking the lattice. The present choice of lattice parameters represents a choice, in the absence of tracking results, to go with parameters that make the magnet parameters easier to achieve and provides increased protection from energy deposition due to showers coming from the long straight sections; however, it is entirely possible that we will have to compromise these goals somewhat in order to achieve good enough dynamic aperture.

1.4 Beam Induced Energy Deposition And Radiation Fields

N. Mokhov

Discussion similar to Study–I.

Arc Magnets N. Mokhov

This section is different from Study–I to the extent that the open coil structure adopted for Study–II changes the energy deposition pattern. Some mitigation of hot spots still might be required. An important result here is the extent to which the warm cells near then ends of the arcs are useful in trapping energy coming from the long straight sections.

Straight Section Components N. Mokhov

Estimations for energy deposition issues for warm magnets, kickers, diagnostics etc. This also may be the best pace to discuss protection against injection errors and injection tuning. If a superconducting rf system is needed then there may be issues for how to protect and isolate it. In particular it may not be possible to use windows to isolate the rf station's beam vacuum (unlike previous accelerator).

Radiation Around Arc Tunnel And Downstream Of Straight Sections N. Mokhov

Standard discussion but takes into account BNL guidelines.

2 REFERENCES

[1] Semertzidis and Morse paper.

[2] BST paper from the 1989 ICFA beam Dynamics Workshop.